ETHZ-IMP-PR-92-5
Fermilab Library
0 1160 0013981 0

ETHZ-IMP PR/92-5
July 1992

FERMILAB
JUL 22 1992
LIBRARY

Studies of Helium Gas Mixtures as a Drift Chamber Gas

Christoph Grab

Institute for Intermediate Energy Physics, ETHZ,
ETH-Hönggerberg, CH-8093 Zürich, Switzerland

Contribution to:
"B-Factories: The State of the Art in Accelerators, Detectors and Physics"
Stanford Linear Accelerator Center, Stanford, CA
April 6–10, 1992

ROUTE TO

NAME	LOCATION
~~Denisov~~	352

Institute for
Intermediate Energy Physics
ETH Zurich
ETH-Hönggerberg

8093 Zürich
Switzerland

Studies of Helium Gas Mixtures as a Drift Chamber Gas †

Christoph Grab
Swiss Federal Institute of Technology, ETHZ, 8093 Zürich, Switzerland

ABSTRACT

Helium gas mixtures have been shown to improve the momentum resolution for tracking of particles with momenta below 1 GeV/c, because of the reduction in multiple scattering. An overview on a series of measurements carried out with several interesting Helium gas mixtures, including Helium-Dimethylether and Helium-Isobutane, is presented. In particular, drift velocities, spatial resolutions, momentum resolution and differential energy loss dE/dx are covered. The measurements were done by means of a small drift-chamber with a drift region of up to 8 cm, operated at atmospheric pressure with electric fields of around 560 V/cm.

1. Introduction

A series of studies of gas mixtures of Helium (He) and organic compounds to serve as a drift chamber gas in experimental surroundings typical of detectors at B-factories has been performed. Detailed descriptions of the measurements can be found in ([1], [2], [3], [4] and [5]). The aim was to measure the different properties and to find a mixture that would be adequate to cover the needs for an intermediate tracking device, such as a large jet drift chamber. This requires providing good momentum resolution for particles of momenta from around 50 MeV/c up to approximately 2.5 GeV/c. In addition, such a gas chamber should yield information about the specific energy loss dE/dx for particle identification. The choice of Helium as the primary gas is explained below. Because pure He is not a usable gas, organic admixtures in several different ratios, such as Isobutane (iC_4H_{10}), Dimethylether (DME) and CO_2 were studied. We adhere to the notation AB$\alpha\beta$, where A and B denote the gases used, and α and β give their relative ratio in units of 10%.

2. Properties of Helium

The choice of Helium as the primary gas is due to its distinct properties, and largely influences the behaviour of the chamber. Not all properties are of course desirable, and some of the effects are intentionally altered by the choice of the secondary organic gas.

First and most importantly, Helium has a very *large radiation length* X_0 of 5284 m, which is of importance for the reduction in multiple scattering in the chamber, and hence leads to increased momentum resolution (see table 1). The *low drift velocity* of He (< 10mm/μm) leads to large drift times t_D and thus better position resolution. This can be a drawback for cases where fast information is essential, e.g. for triggering purposes.

He results in a *low primary ionization*, i.e. the number of primary ion pairs N_P is around 4.2 pairs/cm. Therefore large fluctuations dominate the position resolution at short drift distances. Operating the chamber at a higher gain would help, but this shortens the operating plateau. One finds that for both good momentum resolution σ_P and good particle identification by energy loss measurements, a minimal N_P of around 15 pairs/cm is needed. According to earlier measurements [8], however, already very small contaminations (or admixtures on the order of a few parts per 10^4) to pure He can increase the N_P by up to 50%. The reason is that any other molecule (except Ne) has a very high chance of being ionized through the Penning effect, $He^* + A \rightarrow He + A^+ + e^-$, as the He has high

† The contributions of R.Bernet, R.A.Eichler, S.Playfer, B.Stampfli, and I.-A.Yadigaroglu are gratefully acknowledged.

Table 1: Properties of Gases and Mixtures [6,7]:

Gas Mixture	Ratio	X_0 [m]	N_P [cm^{-1}]
Helium	100:0	5284	4.2
Argon		110	24.3
CO_2		183	36.5
C_2H_6		340	51
iC_4H_{10}		169	93
DME (C_2H_6O)		222	62
Ar:C_2H_6	50:50	166	37.7
CO_2:iC_4H_{10}	90:10	181	42.2
He:iC_4H_{10}	90:10	1313	13.1
	80:20	749	22.0
	70:30	524	30.8
He:CO_2:iC_4H_{10}	80:10:10	776	16.3
	70:20:10	550	19.5
He:DME	90:10	1612	10.0
	80:20	951	15.8
	70:30	674	21.5

lying metastable states of 19.8 and 20.6 eV. Hence, in realistic experimental environments, the N_P may be higher than expected.

Unfortunately, He possesses a *large single electron diffusion* D of 580 $\mu m/\sqrt{cm}$, and pure He has essentially *no quenching* property.

The addition of organic gases compensates in particular the last three mentioned disadvantages of He (N_P, D and quenching). A calculation [9] of the diffusion as a function of the mixing ratio for various gases is shown in fig.1 of ref. [5]. The large diffusion of He decreases very fast; an admixture of only 10% already reduces D by a factor of two, and for more than about 30% of organic components, the diffusion becomes nearly independent of the ratio and just reflects the organic gas properties.

Furthermore, He has a very *low photon absorption cross-section* σ_{PA}, making it less sensitive to backgrounds such as synchrotron radiation. Last, He has a *small Lorentz angle* and is *UV transparent.*

3. Measurements

3.1 Overview

A series of experiments were done at ETH Zürich and at PSI (Paul Scherrer Institute) to study gas properties using a small drift chamber with a jet-type cell geometry. With a nitrogen laser a well defined beam at precisely controlled drift distances was produced. This allowed to map out the time-to-distance relation of a particular gas at different electric fields, and to extract from this the drift velocity v_D. Cosmic ray particles, incident within a restricted angular range, provide a source of MIP's to determine the spacial resolution σ_X as a function of drift distance x_D. With a standard ^{55}Fe source (5.9 keV photons) the gas gain was calibrated, and measurements of the γ-absorption rate were done.

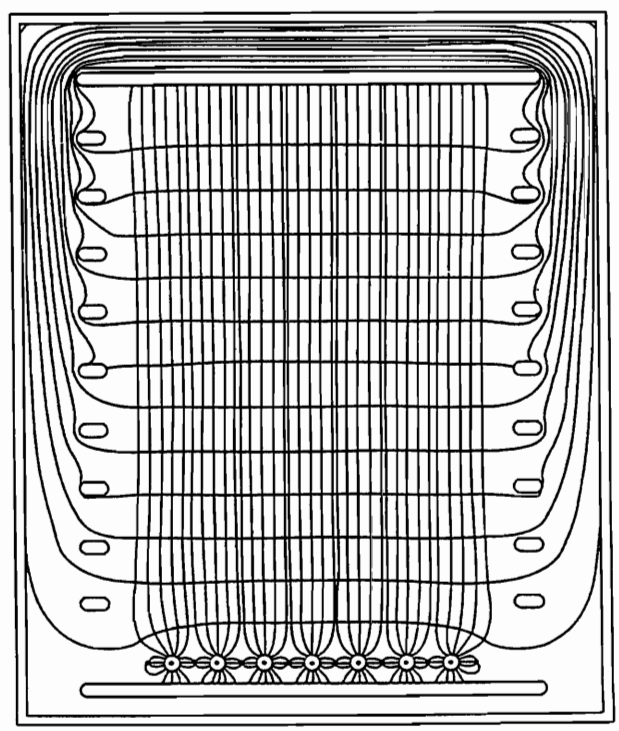

Figure 1: Field geometry of the chamber : Electron drift and equipotential lines.

Finally, particle beams of π, μ and electrons at momenta of 115, 200 and 409 MeV/c were used to measure the specific ionization loss dE/dx as a function of the velocity (β, resp. $\beta \cdot \gamma$). This allows the determination of the particle separation power of a gas mixture.

3.2 Apparatus

The chamber is a small planar drift chamber of 10 x 10 cm^2 active area with a geometry that is similar to a typical jet chamber cell structure. Figure 1 shows the field geometry of the chamber, as calculated by the WIRCHA program [9].

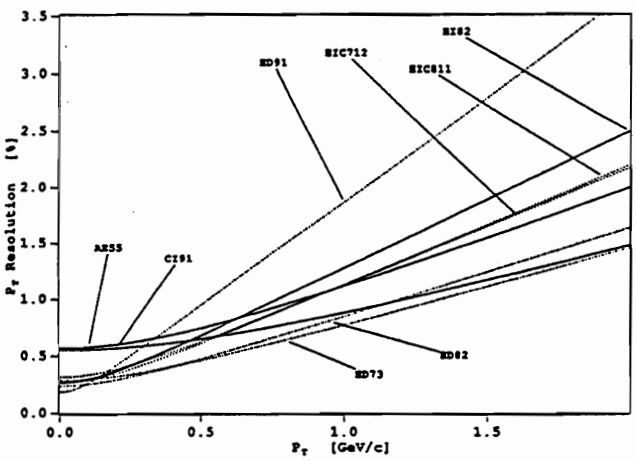

Figure 2: Resolution of transverse momentum, calculated from the measured position resolution (see text)

Eight anode wires, spaced by 8 mm, and a set of field shaping electrodes provide a uniform drift region of up to 8 cm. The overall alignment precision is better than 100 μm. Typical operating conditions are : cathode plane at -5 kV, anodes at +1.6 kV, field wires at -200 V; this produces a drift field of typically 560 V/cm and a gas gain around 10^5 (which was optimized for the σ_x measurements). Particles entered the chamber through a thin quartz window and traversed the active chamber region at a constant distance x_D to the anode wires.

The gas system was computer controlled and allowed a mixing accuracy well below the 1% level. The chamber could be evacuated down to less than 5 mbar. The chamber (volume of 3 l) was supplied with gas at a flow rate of typically 0.1 to 0.5 l/min.

For the data-acquisition we used the components developed for the H1-experiment at HERA. This includes the preamplifier mounted directly on the chamber endplate (gain of 110 mV/μA, 10 ns rise-time, noise level of 2.5 mV), the FADC-card in a VME-crate (100 MHz, 8 bit non-linear with 2.56μs memory) and the readout controller. The data were readout via VME by a Macintosh computer. Triggering was done by means of standard NIM electronics, where in general a coincidence was required between the central anode wire and either a photodiode (laser calibrations), the scintillators (cosmic rays) or the beam hodoscope (dE/dx measurements).

4 Results

Drift velocity: With the nitrogen laser (λ = 337.1 nm, pulse length 500 ps) the drift region was mapped in 5 mm steps from 6 mm to 60 mm. The beam size in the chamber was below the 250 μm intrinsic resolution and its ionization typically five times that of a minimum ionizing particle (MIP). The t_0 and corrections were determined and then the $t_D - x_D$ relation measured for the different mixtures. For drift distances x_D above 1 cm, $t_D - x_D$ is found to be linear, hence we quote the slopes of $t_D - x_D$ as drift velocity v_D. The resulting v_D are in agreement with values measured by other groups [10] [11] [12], and with calculations e.g. by Biagi [12] or Fehlmann [9]. Our drift fields were well below the E=2 kV/cm region, where one would expect saturation effects for v_D to become important.

Spacial resolution: Cosmic rays, triggered by means of scintillators located above and below the chamber (in coincidence), serve for the position resolution measurement. σ_x is obtained from the position-residua of the central anode wire by performing a straight line fit through the data points of the other N wires. The resulting function is fitted to the form $\sigma^2(x) = \sigma_0^2 + \sigma_1^2 \cdot x$, where σ_0 reflects the effects of ionization statistics, electronics, systematics in $t_D - x_D$ etc., and σ_1 mainly describes the contribution from the single electron diffusion. To quote typical values, the average of x_D between 1 and 3 cm is given as σ_2(x). We find σ_2(HD) typically around 150 μm, σ_2(HI) $\approx$ σ_2(HIC) $\approx$ 200μm. At very small x_D, deviations from above parametrization were found. The full table of all measured σ_0 and σ_1 can be found in [2]. As an example, HD82 has $\sigma_0 = 60 \pm 20\mu$m, $\sigma_1 = 99 \pm 6\mu$m, which leads to a $\sigma_2 = 152 \pm 7\mu$m for E=562 V/cm.

Momentum resolution: To calculate the momentum resolution ($\Delta p/p$), we apply the Glückstern formula [13] (first order only) to reflect the influence of the position resolution, and add the first order term for

the multiple scattering (MS) contribution:

$$\frac{\Delta p}{p} = \left(\frac{k_{pos} \cdot \sigma_x}{L^2 \cdot B \cdot \sqrt{n+5}}\right) \cdot p_t + \left(\frac{k_{MS} \cdot \sqrt{\frac{d}{X_0}}}{L \cdot B \cdot \beta}\right)$$

To obtain numbers realistic for a B-factory detector, the following assumptions were made: n=40 aequidistant measuring layers; track length L=50 cm; magnetic field B=1 T; material thickness d in units of radiation length X_0; velocity β; constants k_{pos} = 90 (Tm/GeV) and k_{MS} = 0.05 (Tm). The resolution calculated with our measured values of σ_x is shown in figure 2. We find that compared with a standard Ar:C_2H_6 mixtures, He- mixtures provide better momentum resolution in particular in the low p_t region below 500 MeV/c. At higher p_t , σ_x becomes the dominant limitation and hence He:DME give better resolutions.

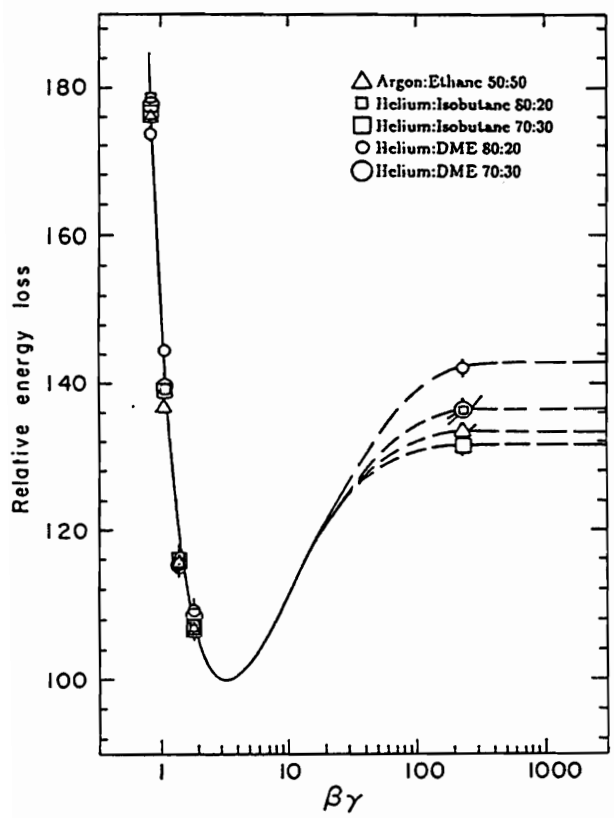

Figure 3: Specific energy loss

γ Absorption rate: The photon absorption properties are measured by illuminating the chamber with a standard ^{55}Fe γ-source of 5.9 keV and recording the rate (i.e. the current) on the anode wires. The results are included in table 2 in arbitrary units (a.u.). Note that the observed rates roughly agree with expectations from the respective photoattenuation lengths. Clearly the He-mixtures are typically one to two orders of magnitude less sensitive to photons (in this energy range). This is an important point of consideration for high background environments, such as high synchrotron radiation.

Specific energy loss dE/dx: Particle beams of pions, muons (from pion decays) and electrons were available at PSI. Three beam momenta, 115, 200 and 409 MeV/c, were chosen such as to provide data points in the different regions of the dE/dx ranges ($1/\beta^2$, minimum ionizing and relativistic rise). The timing was accomplished by means of coincidences of a series of small scintillators with the anode wires. The anode signals, digitized by the FADC, were offline analyzed to obtain the correct total charge per pulse. After linearization, offset correction and integration of individual pulses, the relative gain of the different wires were adjusted. To calculate the specific energy loss (in relative units) the method of truncated mean over 60% of all signals (in our case that is 4 wires) is applied. Particle identification (PID) was done by means of time-of-flight (TOF) measuring the anode pulses with respect to the accelerator radiofrequency. The flight path of particles was 15 m and we achieved a typical PID efficiency of 90%. The correct assignment of the PID method was confirmed independently by a threshold Cerenkov counter (using Aerogel with n=1.055), and a standard absorber-scintillator stack as a range counter. The measured relative width of the specific energy loss distribution (in FWHM/mean) is presented in [4]. It is independent of the absolute gain calibration. To obtain the relative energy loss of the different mixtures for various $\beta \cdot \gamma$ values, the curves were normalized relative to each other at the minimum dE/dx, i.e. at $\beta \cdot \gamma = 3.2$. The shape of the curve in the $1/\beta^2$ region was calculated with the standard Bethe-Bloch formula. The relative gain factors are then extracted from the ratios R(π,p) of measured (dE/dx) for π at momenta p to the calculated (dE/dx) for π at p. Furthermore, we assumed identical gain factors for π, μ and e, i.e. R(π,p) = R(e,p) = R(μ,p). In fact, R(π,p) turned out to be equal to R(μ,p) within 2%.

One figure of merit to compare different gas mixtures in view of particle identification is the particle separation power between electrons and pions,

Table 2: Summary of measurements : The numbers are based on a tracking detector with 40 measuring layers over a radial distance of 50 cm in a magnetic field of 1 Tesla, operated at NTP. The momentum resolution in % is extracted from the measured spatial resolution for a mean drift distance of 2 cm (Glückstern). The measured γ absorption rates are given in arbitrary units. The quoted dE/dx separation power, scaled from 7 to 40 layers, is defined as the difference of the mean dE/dx between electrons at 115 MeV/c and muons at 409 MeV/c, in units of the average width (in σ) of the two.

Gas Mixture	Ratio	Drift Velocity [mm/μs]	Momentum Resolution 100MeV/c σ[%]	Momentum Resolution 1GeV/c σ[%]	5.9 keV γ Absorption [a.u.]	dE / dx Separation Power [σ]
He:iC$_4$H$_{10}$	80:20	20.4	0.30	1.28	59	2.7
	70:30	21.3				2.5
He:CO$_2$:iC$_4$H$_{10}$	80:10:10	16.4	0.29	1.12	120	
	70:20:10	13.6	0.34	1.13	210	
He:DME	80:20	8.4	0.25	0.84	67	2.8
	70:30	5.7	0.30	0.77	93	2.5
CO$_2$:iC$_4$H$_{10}$	90:10	4.6	0.55	0.88	825	
Ar:C$_2$H$_6$	50:50	50.9	0.65	1.10	7500	2.9

SP(e,π), taken at 400 MeV/c momentum, defined as

$$SP(e,\pi) = \frac{dE/dx(e,400) - dE/dx(\pi,400)}{1/2 \cdot (\sigma^2(e,400) + \sigma^2(\pi,400))^{0.5}}$$

For the numbers quoted in table 2 we assume electrons to be in the plateau, i.e. dE/dx(e,400) = dE/dx(e,115), and both pions and muons to be in the minimum at 400 MeV/c, i.e. dE/dx(π,400) = dE/dx(μ,400). Furthermore, our number of samples (7 layers) was scaled to 40 samples, to comply with the same assumptions for a generic B-factory detector as the other numbers in the table.

5. Summary and Conclusions

For the various He mixtures investigated here, the momentum resolutions found are good. In particular, the mixture He:DME(80:20) appears to be a very promising candidate. It yields a $\Delta p_T/p_T$ of 0.25% already at a p_T of 250 MeV/c and reaches 1% at around 1.5 GeV/c. It has a low drift velocity of 8 mm/μs and thus expected drift times are of the order of μs. If the timing aspect of the chamber is crucial, e.g. for triggering purposes, then He:iC$_4$H$_{10}$ provides a faster alternative mixture with only small degradance in resolution performance. Another possibility is a higher drift field, if practical operation considerations allow it, or a change in chamber geometry, such as smaller cells [14].

In terms of particle identification, both He:DME and He:iC$_4$H$_{10}$ are only some 10 to 20% worse than a standard Ar:C$_2$H$_6$ mixture. This fact can in part be accounted for by their lower primary ionization. On the other hand, the measured values are better than expected, which may be traced back to He being a Penning gas, and thus having a larger effective primary ionization than expected. Once more it seems that the purity of the gases is of great importance.

Large drift times may increase the sensitivity to background processes. However, in case of photons e.g. synchrotron radiation and x-rays from beam masks etc., the He component with its low photon absorption is a big advantage. In such cases, CO$_2$ and Ar:C$_2$H$_6$ mixtures should be avoided, being factors of 10 and 100 respectively more sensitive than He:DME(80:20).

References

[1] R. Bernet, Diplomarbeit ETH-Zürich, 1990.

[2] B. Stampfli, Diplomarbeit ETH-Zürich, 1991.

[3] I.-A. Yadigaroglu, Diplomarbeit ETH-Zürich, 1992.

[4] I.-A. Yadigaroglu *et al.*, Contribution to Wire Chamber conference, Vienna, 1992.

[5] S.M.Playfer *et al.*, Nucl. Instr. and Meth. A315, (1992) 494.

[6] F.F.Rieke and W.Prepejchal, Phys. Rev. A6, (1972) 1507.

[7] A.Pansky *et al.*, Proc. Wire Chamber Conf. Vienna, 1992.

[8] W.P.Jesse and J.Sadauskis, Phys. Rev. 100 (1955) 1735.

[9] J.Fehlmann, J.A.Paradiso, G.Viertel; ETH Zürich Internal Report (1983).

[10] V. Cindro, *et al.*, Nucl. Instr. and Meth. A309, (1991) 411.

[11] P. R. Burchat, J. Hiser; SLAC PUB-5626, 1991. submitted to Nucl. Instr. and Meth.
see also J.Va'vra, Nucl. Instr. and Meth. A244, (1986) 391.

[12] J.Va'vra *et al.*, SLAC-PUB-5728, 1992; and Proc. Wire Chamber Conf. Vienna, 1992.

[13] R.Glückstern, Nucl. Instr. and Meth. 24, (1963) 381.

[14] A.Boyarski, *et al.*, Nucl. Instr. and Meth. A283, (1989) 617.
see also: A.Boyarski, these proceedings.